Molekul, Vol. 17. No. 3, November 2022: 436– 446

MOLEKUL
eISSN: 2503-0310

Articles

https://doi.org/10.20884/1.jm.2022.17.3.7017

# Potential Indonesian Natural Compound as antiviral for COVID-19 targeting the RdRp: In silico Study

**Zahra Silmi Muscifa[1], Tony Sumaryada[1], Laksmi Ambarsari[2], Setyanto Tri Wahyudi[1,3]***

[1]Department of Physics, Faculty of Mathematics and Natural Sciences, IPB University, Indonesia 16680
[2]Department of Biochemistry, Faculty of Mathematics and Natural Sciences, IPB University, Indonesia 16680
[3]Tropical Biopharmaca Research Center, Institute of Research and Community Services, IPB University, Indonesia 16128

*Corresponding author email: stwahyudi@apps.ipb.ac.id

**Received** June 09, 2021; **Accepted** October 04, 2022; **Available online** November 20, 2022

**ABSTRACT.** Research related to SARS-CoV-2 drugs is still ongoing. In this initial research, we perform a computational approach on SARS-CoV-2 inhibitors. RNA-dependent RNA polymerase (RdRp) is one of the functional proteins in SARS-CoV-2 that can be a target for drug development, which has an essential function in the viral replication process synthesizing the RNA genome of the virus. This study used the RdRp-Remdesivir complex structure from RCSB with ID PDB 7BV2, with a resolution of 2.5 Å. Currently, Remdesivir is under the clinical trial phase as a Covid-19 drug. In this study, we tested a thousand natural Indonesian compounds used as SARS-CoV-2 RdRp inhibitors obtained from the Indonesian natural compounds database (HerbalDB). The first stage of this computational analysis was pharmacophore modeling structure-based drug design. The natural compounds were analyzed based on their steric and electronic similarities to Remdesivir. A molecular docking simulation was then performed to obtain binding energy and bond stability to produce natural compounds that can inhibit RdRp SARS-CoV-2. The final stage was the molecular dynamics simulation that explored the conformational space of natural compounds and proteins. The ADMET (Absorption, Distribution, Metabolism, Excretion, and Toxicity) test was carried out on the five best compounds to obtain these natural compounds' computational pharmacology and pharmacokinetics. The simulation identified Sotetsuflavone (CID: 5494868) from Cycas revoluta, Grossamide (CID: 5322012) from Cannabis sativa, and 6-Hydroxyluteolin-6,7-disulfate (CID: 13845917) from Lippia nodiflora are the best compounds that can inhibit RdRp SARS-CoV-2. These potential compounds can then be tested in-vitro and in-vivo in the future.

**Keywords**: admet test, docking, Indonesian natural compound pharmacophore modeling, molecular dynamic simulation, SARS-CoV-2.

## INTRODUCTION

Covid-19 has infected over 1.8 million people and killed 50,723 people in Indonesia as of June 2nd, 2021 (Covid19.go.id, 2021). The total confirmed cases increases due to high mobility, making transmission of the SARS-CoV-2 virus difficult to stop. Symptoms of Covid-19 range from asymptomatic to acute respiratory distress syndrome and multi-organ dysfunction. (Subbarao & Mahanty, 2020). Covid-19 is caused by the severe acute respiratory syndrome coronavirus 2 (SARS-CoV-2), a member of the coronavirus family which causes SARS and MERS (Vieira et al., 2020).

Genomic information and pathological characteristics are the basis of the information used to develop SARS-CoV-2 drugs and vaccines (Wu et al., 2020). SARS-CoV-2 has 30,000 nucleotide bases and encodes 29 structural and functional proteins (Zeng et al., 2020). RNA-dependent RNA polymerase (RdRp) is the most conserved protein of the coronavirus replicase-transcriptase. RdRp plays a role in the process of genome replication and transcription of SARS-CoV-2 RNA in new host cells (Naqvi et al., 2020). RdRp is a potential target protein in the development of antiviral drugs for COVID-19.

Natural compounds are traditional medicines that have antiviral and antibacterial properties (Aswatira 2013). The potential of the natural compound as an antiviral for SARS-CoV-2 can be researched and developed. The discovery of a new drug requires a long process. In silico method can perform screening at an early stage regarding drug discovery based on the structure and biological activity of natural compounds and their interactions with the SARS-CoV-2 protein. The inhibitory effect of natural compounds on RdRp can be analyzed from the simulation results' energy affinity (Bhowmik et al. 2020).

Computer simulation can reduce research costs related to pharmaceutical drugs by predicting ligand binding affinity with the receptor active site (Yu & Mac Kerell, 2017). In this computational analysis, molecular docking simulations that can calculate the affinity of ligand bonds with receptors and binding poses to predict the potential of compounds as protein inhibitors were performed (Vieira & Sousa, 2019), and molecular dynamics simulations were also conducted to determine the structural dynamics of protein and ligand complexes in testing potential candidate compounds as potential compounds protein inhibitors (Karplus & McCammon, 2002)

In this study, one thousand structures of Indonesian natural compounds were used in the initial screening stage. The database used in the study comes from the Indonesian natural compounds database (HerbalDB) (http://herbaldb.farmasi.ui.ac.id/v3/) (Syahdi et al., 2019), and the 3D structure is retrieved from Pubchem (https://pubchem.ncbi.nlm.nih.gov/) (Kim et al., 2021). The crystal structure of the RdRp receptor was retrieved from RCSB (https://www.rcsb.org/ ) with the PDB code 7BV2 with a resolution of 2.5 Å. The 7BV2 is a protein complex structure consisting of RdRp SARS-CoV-2 and Remdesivir (Yin et al., 2020). Remdesivir is an adenine nucleotide analog with broad-spectrum antiviral activity against various RNA viruses (Eastman et al., 2020). Remdesivir is the first drug approved by the U.S. Food and Drug Administration (FDA) to treat COVID-19 under an emergency use authorization (U.S food and drug administration, 2020). A study conducted by (Abd-Elsalam et al., 2021) showed that administering remdesivir 200 mg daily for ten days in addition to supportive therapy had significantly shortened hospital stay in the intervention group compared to the control group. In this study, we conduct a computational method to effectively-identified potential Indonesian natural compounds as inhibitors RdRp, which eventually can be developed as a drug for Covid-19 treatment.

## EXPERIMENTAL SECTION

### Phytochemical Database and Virtual Screening

The stages began with constructing a database of 1000 from Indonesian natural compounds database (HerbalDB). First, the phytochemical 3D structure was downloaded from the PubChem database. The next stage was conducting a virtual screening of pharmacophores modeling with structure-based drug design based on the similarity between steric and electronic features of natural compounds with remdesivir using LigandScout 4.4 (One-month free trial) (Wolber and Langer 2005). The structure of the remdesivir used was derived from the complex protein structure found in 7BV2. At this stage, 100 natural compounds with at least four pharmacophoric common features with remdesivir were identified. The stage continued with the optimization and improvement of the structure of the 100 best compounds using Orca. By default, Orca uses a Quasi-Newton optimizer using the Broyden, Fletcher, Goldfarb, and Shanno a second-order optimization algorithm method, and the optimization is carried out in redundant internal coordinates (Neese, 2018). But in this research, we are using approximation based on proposed three-fold corrected Hartree-Fock (PBEh-3c) method (Grimme et al., 2015).

### Docking Simulation

The active compound that had been optimized using Orca was be used as a ligand in the several docking stages. Docking simulation use grid box with coordinates were $x = 94.39$ $y = 91.65$ $z = 104.806$ and size of grid box is $15 \times 15 \times 15$ Å. The first docking simulation was a specific virtual screening based on the bond affinity value of 100 natural compounds to RdRp with Autodock-Vina (Trott & Olson, 2009). This resulted in eleven compounds that showed better binding energy than remdesivir. After that, autogrid parameter files (gpf) and Autodock parameters (dpf) were created for docking using Autodock-4 (Morris et al., 2009), and the third consistency test for the bond energy of five compounds with the lowest binding energy with PSO-vina was also administered (Ng et al., 2015). Visualization of ligand and protein complex structures was performed using the Ligplus software (Laskowski & Swindells, 2011).

### Molecular Dynamics Simulation

Molecular dynamics simulations of the five complex structures of 7BV2-natural ligand and 7BV2-remdesivir compounds as controls are produce using AMBER16 software (Salomon-Ferrer et al., 2013) using GPU (Graphics Processing Unit). The force fields used to run molecular dynamics simulations included ff14SB (Maier et al., 2015), RNA.OL3 (Zgarbová et al., 2011) and GAFF2 (Wang et al., 2004) respectively used for proteins, RNA, and ligands. Neutralization of complex systems was carried out using 0.15 M salt applied to each system. The complex structure was inserted into the water box with a radius of 10 Å. The topology and coordinates files were prepared for minimization using constrained minimization with a 10 kcal $\mathrm{mol}^{-1}\,\mathrm{A}^{-1}$ limit placed on each hydrogen atom and the molecules in the system. Each system undergoes a 50.000-step minimization process. The system temperature gradually increased to 310 K. For the equilibrium process Langevin protocol was used, using an NVT ensemble (fixed volume and temperature), 50.000 steps, and a time step of 2 fs (dt) with a 5 kcal $\mathrm{mol}^{-1}\,\mathrm{A}^{-1}$ limitation. The relaxation process then uses the NPT protocol (fixed pressure and temperature). The equilibration results of the NPT method underwent a 50-ns molecular dynamics simulation with 25 separate scripts using a timestep of 2 fs. Analysis of molecular dynamics simulations was followed by the calculation of Root Mean Square Deviation (RMSD), Root Mean Square Fluctuation (RMSF), hydrogen-bonding interactions, and MMPBSA energy.

### ADMET Test

An ADMET analysis complements this research in collecting information on the absorption, distribution, metabolism, excretion, and toxicity of natural compounds (Yang et al., 2019) as SARS-CoV-2 inhibitors for the pharmacology and pharmacokinetics of these compounds using a web server (http://lmmd.ecust.edu.cn/admetsar2).

## RESULTS AND DISCUSSIONS

### Structure-Based Virtual Screening and Docking Simulation

Structure-based virtual screening is a virtual filter that employs steric information and electronic properties of compounds that have entered the clinical trial stage and have good interactions with target proteins compared to new compounds that are being developed as inhibitors (Klebe, 2006). Remdesivir (**Figure 1.A**) has five pharmacophore features: one ionized to a negative charge shown in red, one aromatic ring shown in purple, two hydrogen-bonding donors shown in red, and one hydrogen-bonding acceptor shown in green. Virtual screening based on pharmacophore features was carried out on a thousand natural compounds. One hundred compounds that had at least four pharmacophoric features in common with remdesivir were obtained.

Several essential residues affect the RNA synthesis process at nsp 12 RdRp SARS-CoV-2. The residue 759-761 binds to two magnesium ions to stabilize the bond between adenosine triphosphate and RdRp SARS-CoV-2. On the other hand, Lys545 and Arg555 interact with the primary strand of RNA to stabilize the triphosphate nucleotide to the right position for the catalysis process (Yin et al., 2020). Other residues play a role in the Ser618 and Ser682 catalytic centers that bind to the 2'OH viral RNA group (Gordon et al., 2020). The statement is in line with Shannon et al. (2020), who mentioned that the main residues of the nsp12 active center include Ser759, Asp760, Asp761, Asp618, and Ser682. Remdesivir competes with nucleotide incorporation and inhibits viral RNA transcription, while the remdesivir phosphate groups obstruct nucleotide access to the active site by occupying the nucleotide entrance (Jiang et al., 2021).

The result of re-docking remdesivir (**Figure 1.B**) showed a hydrogen-bonding interaction between remdesivir and Arg555, Ser759, Asp760, and hydrophobic interactions with residues of Lys 545 and Ser682. The docking result showed that the remdesivir binding location was right in the active site of RdRp SARS-CoV-2 that has four pharmacophoric features in common with remdesivir, which are docked to SARS-CoV-2's RdRp active catalytic center. One hundred natural compounds from docking results also indicated an interaction between active residue and template RNA.

**Table 1** shows the 11 compounds with the lowest energy affinity for docking resulted from molecular docking and remdesivir as a comparison, it can be seen 11 compounds had lower bond affinity values than remdesivir. The difference in the order of binding energy values from Autodock-vina and Autodock-4 is that there is a difference in the scoring function between the two programs. Autodock-vina has the advantage of a much faster docking process and better prediction of binding poses when compared to Autodock-4. Overall, Autodock-4 provides an accuracy of affinity energy values correlated with experimental data (Nguyen et al., 2020).

Remdesivir energy affinity is -6.52 kcal/mol was lower than the best five compounds docked with Autodock-4. Compounds with the best affinity were then sorted by Ligand 1 (L1) to Ligand 5 (L5) and then checked by PSO-Vina for bond stability. The docking was performed 1000 times (**Figure 2**), and the effects of the docking showed the consistency of good affinity energy values.

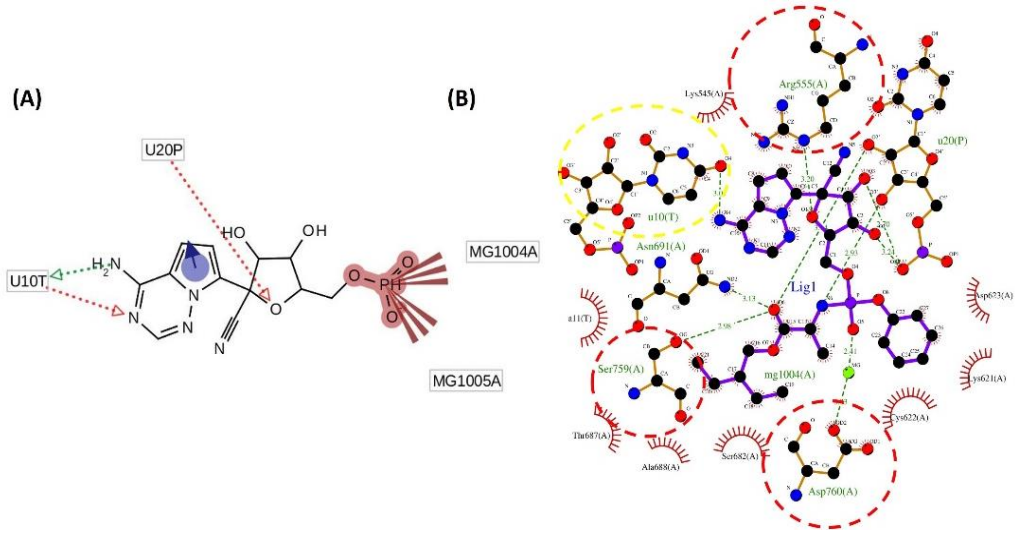


**Figure 1.** (A) Analysis of the pharmacophore properties of remdesivir. (B) Structure of Remdesivir-RdRp Complex

**Table 1** Pharmacophore feature and affinity Energy docking from Autodock-Vina

| No | Compound or Pubchem ID | Pharmacophore Feature | | | | | Vina Energy Affinity (kcal/ mol) | ADT4 Energy Affinity (kcal/ mol) |
|---|---|---|---|---|---|---|---|---|
| | | Ionized to form a negative charge | Aromatic ring | Hydrogen-bonding donors 1 | Hydrogen-bonding donors 2 | Hydrogen-bonding acceptor | | |
| 1 | 5494868 | | ✓ | ✓ | ✓ | ✓ | -10.5 | -8.94(L1) |
| 2 | 65056 | | ✓ | ✓ | ✓ | ✓ | -9.9 | -6.54 |
| 3 | 44260049 | | ✓ | ✓ | ✓ | ✓ | -9.8 | -3.92 |
| 4 | 5322012 | | ✓ | ✓ | ✓ | ✓ | -9.6 | -7.87(L4) |
| 5 | 44256941 | ✓ | ✓ | ✓ | | ✓ | -9.3 | -3.97 |
| 6 | 13845917 | ✓ | ✓ | ✓ | | ✓ | -8.9 | -6.8 (L5) |
| 7 | 44259426 | | ✓ | ✓ | ✓ | ✓ | -8.8 | -5.02 |
| 8 | 442851 | | ✓ | ✓ | ✓ | ✓ | -8.8 | -8.32(L2) |
| 9 | 5378285 | | ✓ | ✓ | ✓ | ✓ | -8.8 | -5.88 |
| 10 | 129852708 | | ✓ | ✓ | ✓ | ✓ | -8.7 | -6.44 |
| 11 | 181883 | | ✓ | ✓ | ✓ | ✓ | -8.5 | -8.11(L3) |
| 12 | Remdesivir | ✓ | ✓ | ✓ | ✓ | ✓ | -8.4 | -6.52 |

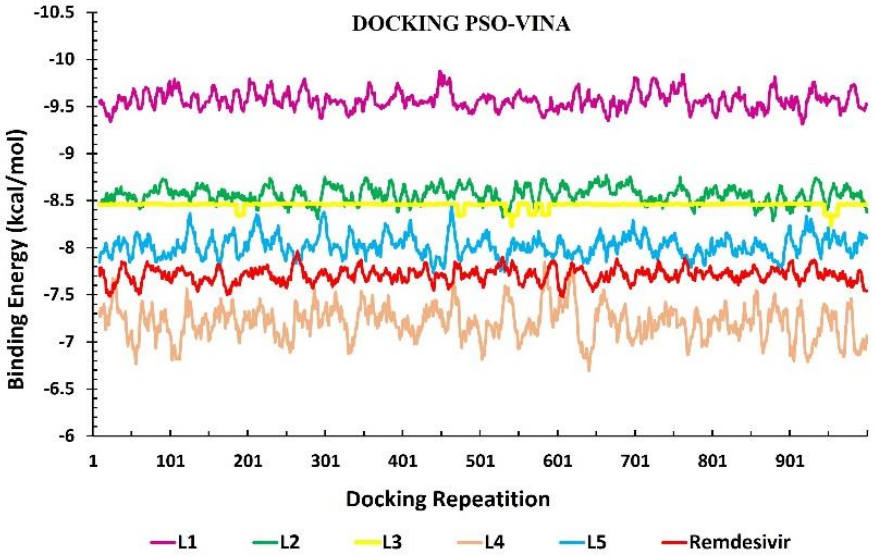


**Figure 2** Consistency of affinity energy using PSO-Vina

## Visual Analysis of Complex Structures

Visual analysis showed that all test ligands had four pharmacophoric features in common with remdesivir. Interaction in the complex structure (**Figure 3** – **Figure 7**) reveals that the ligands had hydrophobic interactions and hydrogen-bonding with the residues present in the active catalytic center and RNA template.

L1 is sotesuflavone from *Cycas revoluta* with Pubchem ID 5494868 with a strong binding affinity with residues in the RdRp catalytic active center, including hydrogen with Arg555, Ser682, Ser759, and the RNA template. L2 is crinasiatine from *Crinum asiaticum* (**Figure 4**) with Pubchem ID 442851, which has single hydrogen-bonding interaction with the residue at the catalytic center of Ser759 and one hydrogen-bonding with the RNA template. L3 is Glycinol II from *Glycine soja* with Pubchem ID 181883 (**Figure 5**) did not show any have hydrogen-bonding interactions with residues at the catalytic center. Instead, two hydrogen-bonding interactions with the RNA template were found. L4 is Grossamide from *Cannabis sativa* with Pubchem ID 5322012 (**Figure 6**) has a one hydrogen-bonding interaction with the residue at the catalytic center, i.e., Ser760 and two hydrogen-bonding encounters with the RNA templates. L5 6-Hydroxyluteolin-6,7-disulfate from *Lippia nodiflora* with Pubchem ID 13845917 (**Figure 7**) have hydrogen bonding with Arg555, Ser682, and one hydrogen-bonding interactions with the RNA template.

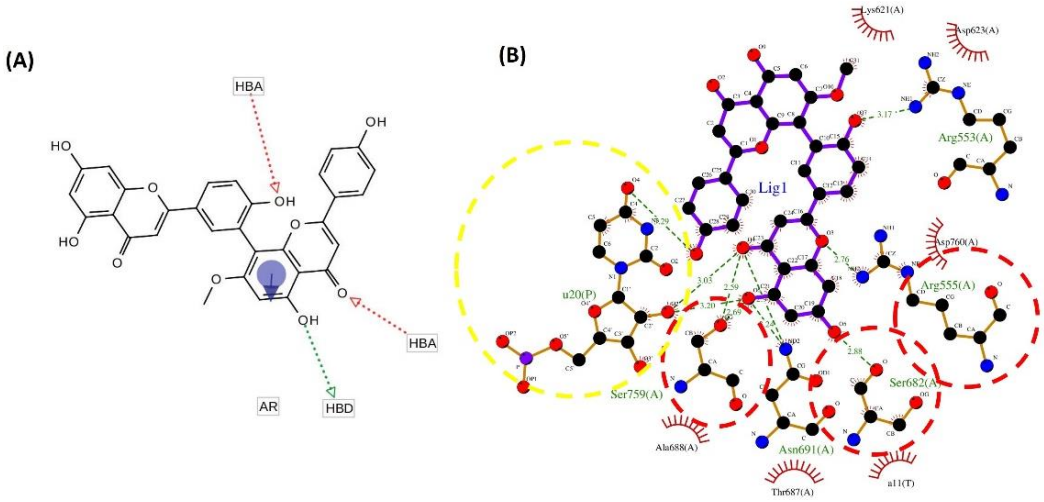


**Figure 3**. (A) Analysis of the pharmacophore features of Ligand 1. (B) Structure of 1-RdRp ligand complex

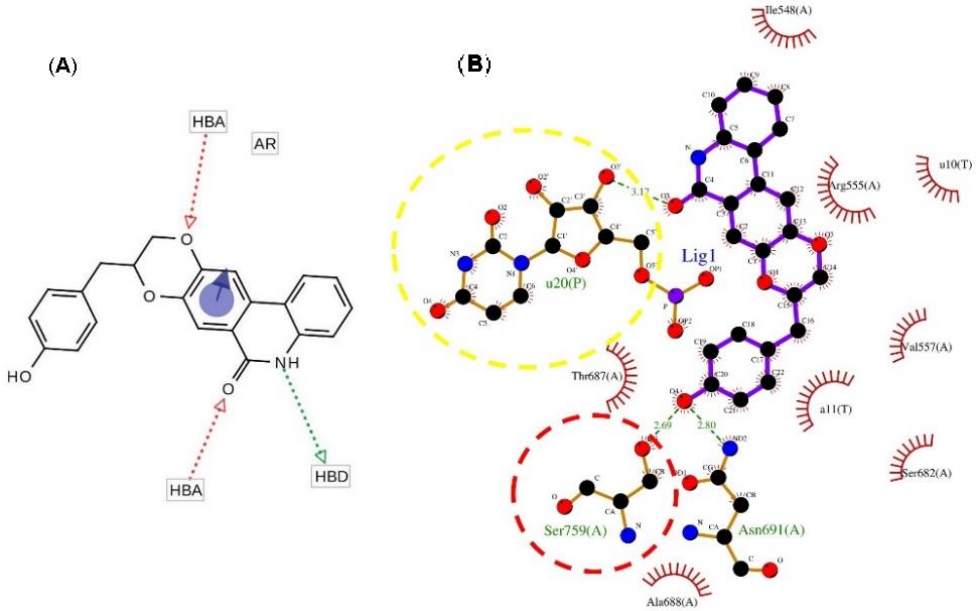


**Figure 4**. (**A**) Analysis of the pharmacophore features of ligand 2. (**B**) Structure of the 2-RdRp ligand complex

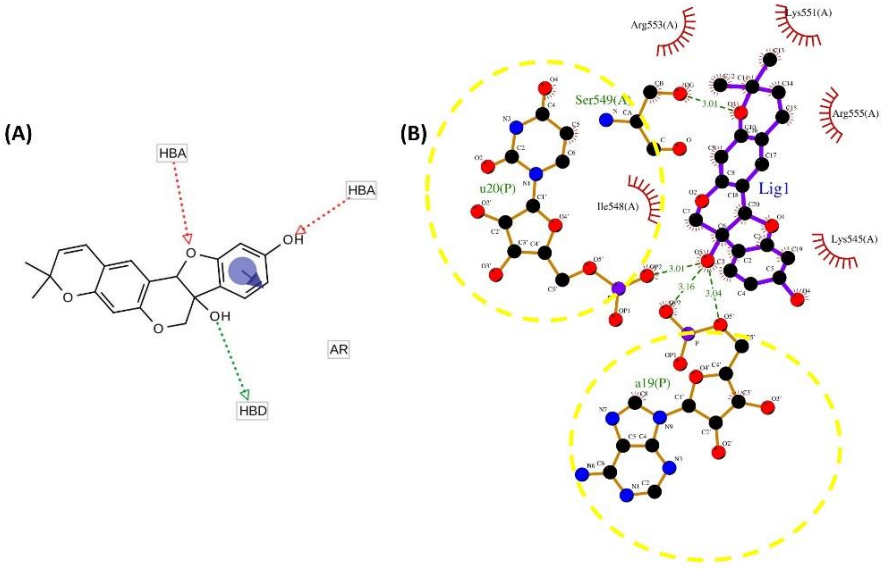


**Figure 5**. (**A**) Analysis of ligand 3 pharmacophore features. (**B**) Structure of the 3-RdRp ligand complex

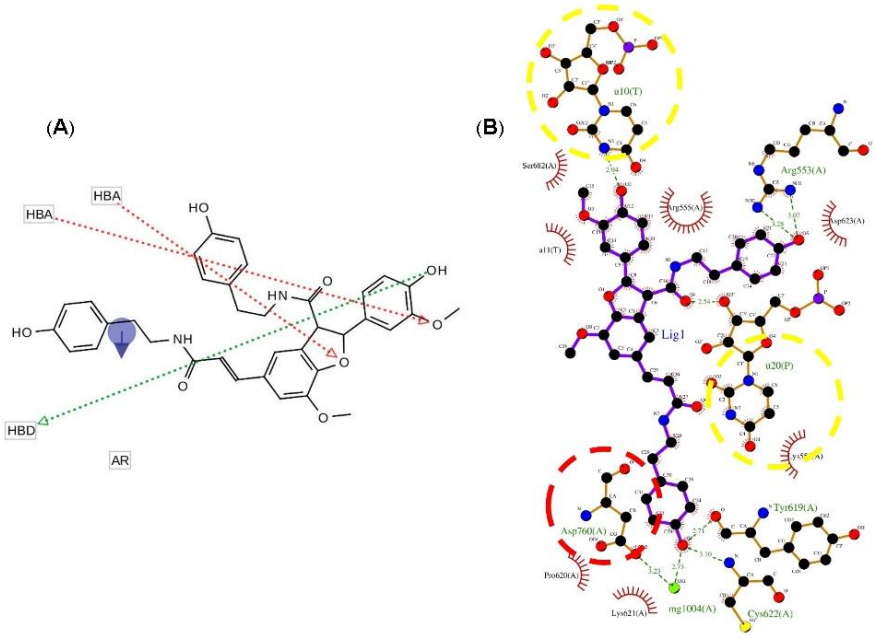


**Figure 6**. (**A**) Analysis of the pharmacophore features of ligand 4. (**B**) Structure of the 4-RdRp ligand complex

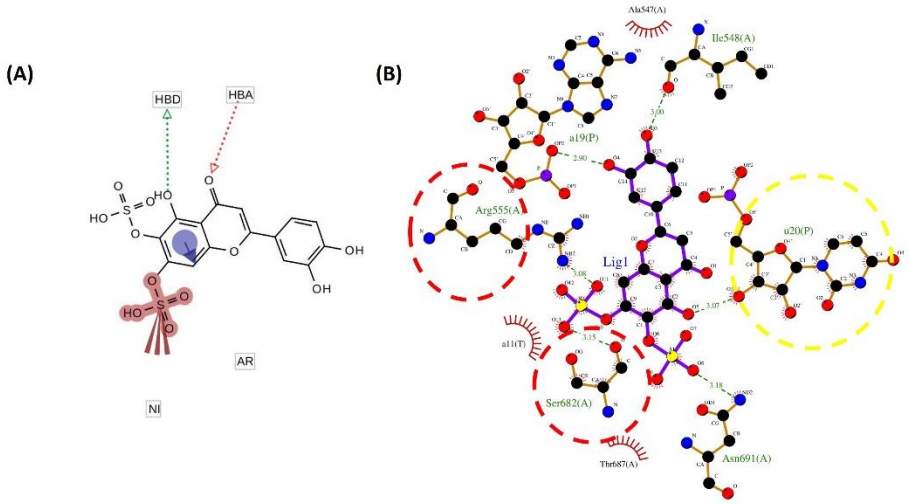


**Figure 7**. (**A**) Analysis of the pharmacophore features of ligand 5. (**B**) Structure of the 5-RdRp ligand complex

## Molecular Dynamics Simulation

The docking approach statistically studies the binding of compounds, while the molecular dynamics simulation approach studies the binding to the active site of a protein as a function of time-integrated with Newton's equations of motion (Adcock & McCammon, 2006). The structural binding of natural compounds and remdesivir on RdRp SARS-CoV-2 can affect the action mechanism of RdRp, affecting its catalytic activity. RMSD data calculations can provide information about the convergence of simulated complex compounds, RNA, and ligands. The RMSD value of the complex structure in **Figure 8A** shows the overall complex structure that converged after 10 ns of simulation.

The complex structure of L2 showed the highest deviation compared to other ligands' complex structures. The mean value of the deviation in all complex structures is ~2Å. Meanwhile, the simulation's RMSD RNA value fluctuated, with an average RMSD of ~1.7 Å. Fluctuations also occurred in the ligand RMSD, with the highest deviation occurring in remdesivir with RMSD ~2 Å while the complex structure of natural compounds showed a deviation of ~1 Å.

The RMSF value (**Figure 9**) shows the fluctuation of amino acid residues in the complex structure during the simulation. In the active side position of Lys545, Arg555, Asp618, Ser682 Ser759, Asp760, and Asp761, the RMSF value was lower than that of the RMSF on other residues. This significant reduction in RMSF value could be attributed to the structural inactivation of RdRp because of the binding of this natural compound and remdesivir at the catalytic site of the RdRp enzyme.

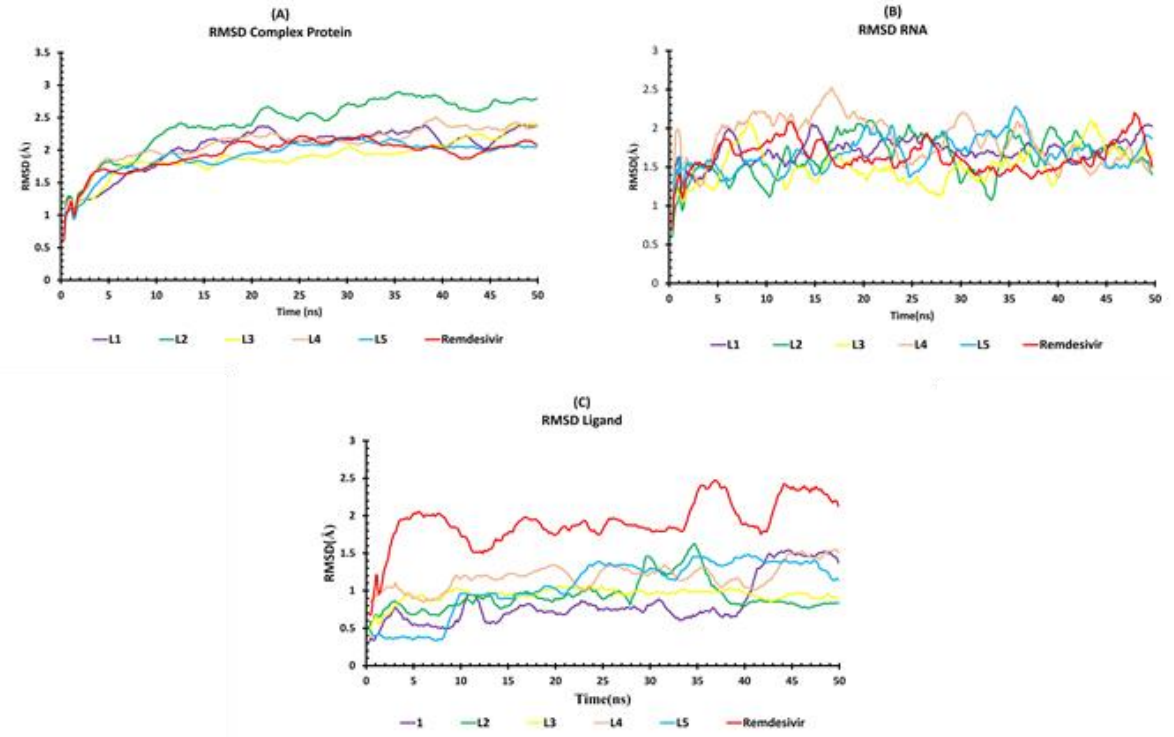


**Figure 8** (**A**) RMSD value of natural compounds and remdesivir. (**B**) RMSD value of complex compound RNA structure. (**C**) RMSD value of complex protein structure

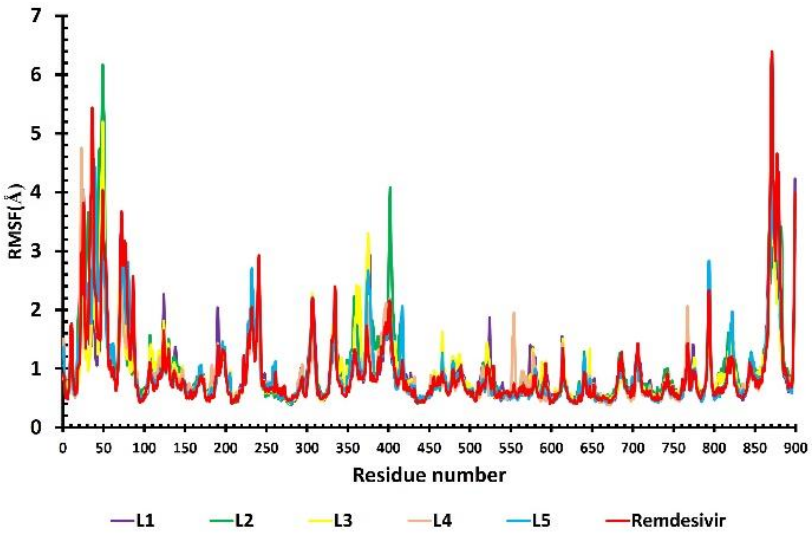


**Figure 9** RMSF value of the complex structure of natural compounds and remdesivir

Analysis of the conformation and stability of the binding structure of RdRp and the subsequent ligand number of hydrogen-bonding can provide information regarding this analysis, providing more insight into the enzyme-ligand binding mechanism. As seen from the number of hydrogen bonding, differences in the appearance of each ligand were found in **Table 2**. The occupancy of hydrogen bonding is the percentage of hydrogen bonding that binds with ligands during the simulation with an average interaction distance of less than 3 Å. The occupancy with high values indicates that the hydrogen bonding between the protein and the ligand increases. During the 50 ns simulation, some residues were on the active catalytic center, binding to ligands with an occupancy value of over 2%.

**Table 3** shows the binding energy of the compound with time as an inhibitor of RdRp, which was measured using the MMPBSA technique. These data can provide information about the stability of the bond between the inhibitor and RdRp as a complex structure.. The total calculation of the binding energy is a combination of electrostatic interactions ($\Delta E_{ELE}$), van der Waals interactions ($\Delta E_{VDW}$), non-polar interactions in a solvated system ($\Delta E_{PB}$), and polar interactions in a solvated system ($\Delta E_{PBSUR}$).

**Table 2**. Residues of RdRp binding to ligands

| Ligand | Donor | Occupancy (%) | Acceptor | Occupancy (%) |
|---|---|---|---|---|
| L1 | Ser759 | 75.6 | Asp618 | 8.8 |
| | Asn691 | 14 | Ser682 | 3.6 |
| | | | Arg555 | 2.4 |
| L2 | Asn691 | 26 | Asn691 | 13.2 |
| | Thr680 | 5.2 | Thr680 | 5.2 |
| L3 | Arg555 | 1.2 | Arg555 | 4 |
| L4 | Gln444 | 6.4 | Phe442 | 85.2 |
| | Cys722 | 5.6 | Ser682 | 49.6 |
| | Arg555 | 1.2 | | |
| L5 | Thr650 | 11.6 | Ser682 | 1.6 |
| | Thr687 | 11.2 | | |
| | Arg555 | 8 | | |
| | Asn691 | 3.6 | | |
| | Lys545 | 4 | | |
| Remdesivir | Ser759 | 31.6 | Asp623 | 37.2 |
| | Asp760 | 14.8 | | |
| | Asp623 | 16.8 | | |

**Table 3**. MMPBSA binding energy for 50 ns captured every 200 frames

| Ligand | ΔEele (Kcal/mol) | ΔEvdw (Kcal/mol) | ΔEPB(Kcal/mol) | ΔEPBSUR(Kcal/mol) | ΔEPBTOT(Kcal/mol) |
|---|---|---|---|---|---|
| L1 | -6.5241 | -46.6172 | 18.694 | -4.872 | -39.3256 |
| L2 | -9.2011 | -40.2917 | 17.0936 | -4.4225 | -36.8271 |
| L3 | -5.7578 | -30.4873 | 11.3537 | -3.4381 | -28.3295 |
| L4 | -13.8887 | -70.3706 | 27.1183 | -7.0253 | -64.1664 |
| L5 | -1.6762 | -39.4084 | 9.9748 | -3.6134 | -34.7232 |
| Remdesivir | -18.9375 | -34.5696 | 24.39 | -4.9017 | -34.109 |

### Testing The ADMETSAR properties

The work was then followed with the ADMET test to determine ADMET (Absorption, Distribution, Metabolism, Excretion, and Toxicity) to determine the pharmacology and pharmacokinetics of these compounds on the webserver http://lmmd.ecust.edu.cn/admetsar2. These indicators are essential in studies related to drug development (Cheng et al., 2012). Five ADMET indicators important in analyzing the Applicability Domain include six physicochemical and topological properties to determine which compound to use. These properties include molecular weight, alogP, number of atoms, number of aromatic rings, number of donors, and acceptors of hydrogen bonding. Human Intestinal absorption is the ability of the drug to absorb into the intestines and digestive system (Wessel & Mente, 2001).

AMES mutagenesis is the ability of drugs to cause mutations that can provide information regarding a compound's toxicity. Carcinogenicity indicates the potential of cancer-causing compounds. The LD50 is the maximum dose in milligrams per kilogram of test animal weight that can cause death in test animals. The ADMET test data from the sample are listed in **Table 4**. Positive and negative signs indicate whether or not it can occur, and decimal values from 0 to 1 indicate the percentage of this occurrence (Guan et al., 2019).

**Table 4** reveals that remdesivir as a control compound has a reasonably strong ADMET indicator. The Applicability Domain Test Indicators, Human Intestinal Absorption, Carcinogenicity show the five best test ligands that can develop as medication have a high percentage of absorbing the intestinal and digestive tract no cancer-causing potential. The AMES mutagenesis test revealed that L2 and L3 have the potential to have toxicity properties for the body because they have a percentage of the potential to cause DNA damage in the bacteria tested.

**Table 4**. Admetsar Properties and Energy Affinity

| AdmetSAR Properties | Remdesivir | L1 | L2 | L3 | L4 | L5 |
|---|---|---|---|---|---|---|
| Applicability Domain | In Domain | In Domain | In Domain | In Domain | In Domain | In Domain |
| Human Intestinal Absorption | (+)0.9135 | (+)0.9889 | (+)0.9882 | (+)0.9881 | (+)0.9771 | (+)0.9545 |
| AMES Mutagenesis | (-)0.7400 | (-)0.6100 | (+)0.7100 | (+)0.5100 | (-)0.6500 | (-)0.5300 |
| Carcinogenicity | Non-carcinogenic | Non-carcinogenic | Non-carcinogenic | Non-carcinogenic | Non-carcinogenic | Non-carcinogenic |
| LD50 In Rat (mol/kg) | 27.169 | 28.336 | 21.936 | 22.823 | 24.651 | 24.496 |
| Autodock-Vina (kcal/mol) | -8.4 | -10.5 | -8.8 | -8.5 | -9.6 | -8.9 |
| Autodock4 (kcal/mol) | -6.41 | -8.94 | -8.33 | -8.11 | -7.97 | -6.46 |
| PSO-Vina Average (kcal/mol) | -7.71 | -9.57 | -8.56 | -8.45 | -7.21 | -8.02 |
| MMPBSA (kcal/mol) | -34.109 | -39.3256 | -36.8271 | -28.3295 | -64.1664 | -34.7232 |

Based on **Table 4**, L1 has a total energy of -39.3256 kcal/mol, L2 has a total energy of -36.827 kcal/mol, L4 has a total energy of -64.1664 kcal/mol, and L5 has a total energy of -34,723 kcal/mol. These results are better than the binding energy of remdesivir, which is -34,109 kcal/mol. This MMPBSA analysis correlated the occupancy of the interaction of the catalytic residue of RdRp SARS-CoV-2 with the ligand (**Table 4**) and was in line with the visual analysis of the docking results with several residues at the catalytic sites Arg555, Ser682, Asn691, Ser759, and Asp760 (**Figure 3** – **Figure 7**). However, from the results of the admetsar test shown in **Table 4**, it can be seen that L2 has a 71% chance of causing DNA damage in the tested bacteria, which has caused L2 is not recommended to be developed as a SARS-CoV-2 inhibitor.

## CONCLUSIONS

It can be concluded that of the 1000 compounds used in this work, sotesuflavone (CID : 5494868), grossamide (CID : 5322012) , and 6-Hydroxyluteolin-6,7-disulfate (CID : 13845917) were the best compounds. These best compounds have four similarities with remdesivir. From the results of docking and molecular dynamics simulations, the best compounds had a better binding affinity and MMPBSA energy than remdesivir. These best compounds also have hydrogen bond interactions with residues in the catalytic center of the protein, which can interfere with the transcription and replication process of RdRp. ADMET testing shows that the best compounds in this study have pharmacological and pharmacokinetic properties like drugs. The three compounds can then undergo in vitro and in vivo tests to confirm their potential inhibition against SARS-CoV-2 RdRp.

## ACKNOWLEDGEMENTS

This work was supported by the Ministry of Research and Technology of Indonesia for a master thesis research scheme (Contract Number. 1/E1/KP.PTNBH/2020).

## REFERENCES

Abd-Elsalam, S., Salama, M., Soliman, S., Naguib, A. M., Ibrahim, I. S., Torky, M., Abd El Ghafar, M. S., Abdul-Baki, E. A. R. M., & Elhendawy, M. (2021). Remdesivir efficacy in Covid-19 treatment: a randomized controlled trial. *American Journal of Tropical Medicine and Hygiene*, *106*(3), 886–890. https://doi.org/10.4269/ajtmh.21-0606

Adcock, S. A., & McCammon, J. A. (2006). Molecular dynamics: Survey of methods for simulating the activity of proteins. *Chemical Reviews*. *106*, 1589-1615, https://doi.org/10.1021/cr040426m

Cheng, F., Li, W., Zhou, Y., Shen, J., Wu, Z., Liu, G., Lee, P. W., & Tang, Y. (2012). admetSAR: A Comprehensive Source and Free Tool for Assessment of Chemical ADMET Properties. *Journal of Chemical Information and Modeling*, *52*(11), 3099–3105. https://doi.org/10.1021/ci300367a

Covid19.go.id. (2021). *Situation of the COVID-19 virus in Indonesia. Accessed April 30*.

Gordon, C. J., Tchesnokov, E. P., Woolner, E., Perry, J. K., Feng, J. Y., Porter, D. P., & Götte, M. (2020). Remdesivir is a direct-acting antiviral that inhibits RNA-dependent RNA polymerase from severe acute respiratory syndrome coronavirus 2 with high potency. *Journal of Biological Chemistry*. *295*(20), 6785-6797. https://doi.org/10.1074/jbc.RA120.013679

Grimme, S., Brandenburg, J. G., Bannwarth, C., & Hansen, A. (2015). Consistent structures and interactions by density functional theory with small atomic orbital basis sets. *Journal of Chemical Physics*, *143*(5), 0–19. https://doi.org/10.1063/1.4927476

Guan, L., Yang, H., Cai, Y., Sun, L., Di, P., Li, W., Liu, G., & Tang, Y. (2019). ADMET-score-a comprehensive scoring function for evaluation of chemical drug-likeness. *MedChemComm*. *10*(1), 148–157. https://doi.org/10.1039/C8MD00472B

Jiang, Y., Yin, W., & Xu, H. E. (2021). RNA-dependent RNA polymerase: Structure, mechanism, and drug discovery for COVID-19. *Biochemical and Biophysical Research Communications*, *538*, 47–53. https://doi.org/10.1016/j.bbrc.2020.08.116

Karplus, M., & McCammon, J. A. (2002). Molecular dynamics simulations of biomolecules. *Nature Structural Biology*. *35*(6), 321-323. https://doi.org/ 10.1038/nsb0902-646

Kim, S., Chen, J., Cheng, T., Gindulyte, A., He, J., He, S., Li, Q., Shoemaker, B. A., Thiessen, P. A., Yu, B., Zaslavsky, L., Zhang, J., & Bolton, E. E. (2021). PubChem in 2021: new data content and improved web interfaces. *Nucleic Acids Research*. *49*(D1), D1388–D1395. https://doi.org/10.1093/ nar/gkaa971

Klebe, G. (2006). Structure-based Drug Design. In *Encyclopedic Reference of Genomics and Proteomics in Molecular Medicine*. (pp. 1816–1818). Springer Berlin Heidelberg. https://doi.org/10.1007/3-540-29623-9_0980

Laskowski, R. A., & Swindells, M. B. (2011). LigPlot+: Multiple ligand-protein interaction diagrams for drug discovery. *Journal of Chemical Information and Modeling*. *51*(10), 2778-2786 https://doi.org/10.1021/ ci200227u

Maier, J. A., Martinez, C., Kasavajhala, K., Wickstrom, L., Hauser, K. E., & Simmerling, C. (2015). ff14SB: Improving the Accuracy of Protein Side Chain and Backbone Parameters from ff99SB. *Journal of Chemical Theory and Computation*. *11*(8), 3696–3713. https://doi.org/10.1021/acs.jctc.5b00255

Morris, G. M., Ruth, H., Lindstrom, W., Sanner, M. F., Belew, R. K., Goodsell, D. S., & Olson, A. J. (2009). Software news and updates AutoDock4 and AutoDockTools4: Automated docking with selective receptor flexibility. *Journal of Computational Chemistry*. *30*(16), 2785-91. https://doi.org/ 10.1002/jcc.21256

Naqvi, A. A. T., Fatima, K., Mohammad, T., Fatima, U., Singh, I. K., Singh, A., Atif, S. M., Hariprasad, G., Hasan, G. M., & Hassan, M. I. (2020). Insights into SARS-CoV-2 genome, structure, evolution, pathogenesis and therapies: Structural genomics approach. *Biochimica et Biophysica Acta - Molecular Basis of Disease*. *1866*(10),165878. Elsevier B.V. https://doi.org/10.1016/j.bbadis.2020.165878

Neese, F. (2018). Software update: the ORCA program system, version 4.0. *WIREs Computational Molecular Science*, *8*(1), e1327. https://doi.org/https://doi.org/10.1002/wcms.1327

Ng, M. C. K., Fong, S., & Siu, S. W. I. (2015). PSOVina: The hybrid particle swarm optimization algorithm for protein-ligand docking. *Journal of Bioinformatics and Computational Biology*. *13*(3), 1541007. https://doi.org/10.1142/S0219720015410073

Nguyen, N. T., Nguyen, T. H., Pham, T. N. H., Huy, N. T., Bay, M. Van, Pham, M. Q., Nam, P. C., Vu, V. V., & Ngo, S. T. (2020). Autodock Vina Adopts More Accurate Binding Poses but Autodock4 Forms Better Binding Affinity. *Journal of Chemical Information and Modeling*. *60*(1), 204-211. https://doi.org/10.1021/acs.jcim.9b00778

Salomon-Ferrer, R., Götz, A. W., Poole, D., Le Grand, S., & Walker, R. C. (2013). Routine microsecond molecular dynamics simulations with AMBER on GPUs. 2. Explicit solvent particle mesh ewald. *Journal of Chemical Theory and Computation*. *9*(9), 3878-3888. https://doi.org/10.1021/ct400314y

Shannon, A., Le, N. T.-T., Selisko, B., Eydoux, C., Alvarez, K., Guillemot, J.-C., Decroly, E., Peersen, O., Ferron, F., & Canard, B. (2020). Remdesivir and SARS-CoV-2: Structural requirements at both nsp12 RdRp and nsp14 Exonuclease active-sites. *Antiviral Research*, *178*, 104793. https://doi.org/10.1016/j.antiviral.2020.104793

Subbarao, K., & Mahanty, S. (2020). Respiratory Virus Infections: Understanding COVID-19. *Immunity*, *52*(6), 905–909. https://doi.org/10.1016/j.immuni.2020.05.004

Syahdi, R. R., Iqbal, J. T., Munim, A., & Yanuar, A. (2019). HerbalDB 2.0: Optimization of Construction of Three-Dimensional Chemical Compound Structures to Update Indonesian Medicinal Plant Database. *Pharmacognosy Journal*, *11*(6), 1189-1194

Trott, O., & Olson, A. J. (2009). AutoDock Vina: Improving the speed and accuracy of docking with a new scoring function, efficient

optimization, and multithreading. *Journal of Computational Chemistry*. 31(2), 455–461. https://doi.org/ 10.1002/jcc.21334

U.S food and drug administration. (2020). *FDA Approves First Treatment for COVID-19*. October 22, 2020. https://www.fda.gov/ news-events/ press-announcements/fda-approves-first-treatment-covid-19

Vieira, L. M. F., Emery, E., & Andriolo, A. (2020). Covid-19: Laboratory diagnosis for clinicians. An updating article. *Sao Paulo Medical Journal*. *138*(3), 259-266. https://doi.org/10.1590/ 1516-3180.2020.0240.14052020

Vieira, T. F., & Sousa, S. F. (2019). Comparing AutoDock and Vina in ligand/decoy discrimination for virtual screening. *Applied Sciences (Switzerland)*. *9*(21), 4538. https://doi.org/ 10.3390/app9214538

Wang, J., Wolf, R. M., Caldwell, J. W., Kollman, P. A., & Case, D. A. (2004). Development and testing of a general Amber force field. *Journal of Computational Chemistry*. *25*(9), 1157-74. https://doi.org/ 10.1002/jcc.20035

Wessel, M. D., & Mente, S. (2001). Chapter 25. ADME by computer. *Annual Reports in Medicinal Chemistry*, *36*, 257–266. https://doi.org/ 10.1016/s0065-7743(01)36065-7

Wu, C., Liu, Y., Yang, Y., Zhang, P., Zhong, W., Wang, Y., Wang, Q., Xu, Y., Li, M., Li, X., Zheng, M., Chen, L., & Li, H. (2020). Analysis of therapeutic targets for SARS-CoV-2 and discovery of potential drugs by computational methods. *Acta Pharmaceutica Sinica B*, *10*(5), 766–788. https://doi.org/10.1016/j.apsb. 2020.02.008

Yang, H., Lou, C., Sun, L., Li, J., Cai, Y., Wang, Z., Li, W., Liu, G., & Tang, Y. (2019). AdmetSAR 2.0: Web-service for prediction and optimization of chemical ADMET properties. *Bioinformatics*. *35*(6), 1067-1069 https://doi.org/10.1093/ bioinformatics/bty707

Yin, W., Mao, C., Luan, X., Shen, D. D., Shen, Q., Su, H., Wang, X., Zhou, F., Zhao, W., Gao, M., Chang, S., Xie, Y. C., Tian, G., Jiang, H. W., Tao, S. C., Shen, J., Jiang, Y., Jiang, H., Xu, Y., … Xu, H. E. (2020). Structural basis for inhibition of the RNA-dependent RNA polymerase from SARS-CoV-2 by remdesivir. *Science*. *368*(6498), 1499-1504. https://doi.org/ 10.1126/ science.abc1560

Yu, W., & MacKerell Jr, A. D. (2017). Computer-Aided Drug Design Methods. *Methods in Molecular Biology (Clifton, N.J.)*, *1520*, 85–106. https://doi.org/10.1007/978-1-4939-6634-9_5

Zeng, W., Liu, G., Ma, H., Zhao, D., Yang, Y., Liu, M., Mohammed, A., Zhao, C., Yang, Y., Xie, J., Ding, C., Ma, X., Weng, J., Gao, Y., He, H., & Jin, T. (2020). Biochemical characterization of SARS-CoV-2 nucleocapsid protein. *Biochemical and Biophysical Research Communications*, *527*(3), 618–623. https://doi.org/10.1016/ j.bbrc.2020.04.136

Zgarbová, M., Otyepka, M., Sponer, J., Mládek, A., Banáš, P., Cheatham, T. E. 3rd, & Jurečka, P. (2011). Refinement of the Cornell et al. Nucleic Acids Force Field Based on Reference Quantum Chemical Calculations of Glycosidic Torsion Profiles. *Journal of Chemical Theory and Computation*, *7*(9), 2886–2902. https://doi.org/10.1021/ct200162x